

LoRa on the Move: Performance Evaluation of LoRa in V2X Communications

Yuke Li¹, Shuangshuang Han², Linyao Yang¹, Fei-Yue Wang³, Hui Zhang⁴

Abstract—Recent years have witnessed much interest in Low Power Wide Area (LPWA) technologies, which are gaining unprecedented momentum and commercial interest towards the realisation of the Internet of Things (IoT). Long Range (LoRa), as a representative LPWA technology, has the potential to satisfy the growing demand for the longer range and larger amount connectivities in vehicular communication networks. In this paper, LoRa is firstly applied into two typical vehicular networks, namely Vehicle-to-Infrastructure (V2I) and Vehicle-to-Vehicle (V2V), and performance of LoRa schemes with different parameter configurations are evaluated and compared. Further, Monte Carlo simulations indicate that the schemes equipped with higher bandwidth or lower spreading factor exhibit significant advantages in combating the fast fading caused by Doppler effect in V2X networks.

I. INTRODUCTION

Internet of Vehicles (IoV), as an indispensable part of IoT, is expected to be the next frontier for automotive revolution and the key of the evolution of next generation intelligent transportation systems (ITS) [1]. V2X communications, as a significant component of IoV, is envisioned to empower the ITS by helping “extend a vehicle’s field of vision” [2], [3]. Today’s intelligent vehicles rely on a mass of sensors to obtain the information of surroundings, and are expected to evolve to be “PARallel VEHICLES” [4], which enables real-time interaction and optimization of the physical vehicles and the artificial ones. This helps to significantly improve driving safety and reduce single vehicle’s cost [5]–[9]. With the sharp increase in the number of vehicles, V2X communications urgently call for a new paradigm to fulfill its growing requirements for connectivity, mainly with

regards to supporting for a massive number of devices, low deployment cost, extended coverage, low device cost and long battery life.

Therefore, low power wide area networks (LPWANs) have attracted much attention from both academia and industry due to their key performance metrics that are energy efficiency, scalability and coverage. They are continuously gaining momentum as fundamental enablers of the IoT paradigm. There are many candidates that have been pushed into global markets by several competing technology providers, such as LoRa [10], Sigfox [11], Narrowband IoT (NB-IoT) [12], and Ingenu [13], etc. LPWANs are ideal for many IoT applications, such as smart cities [14], smart grid [15], and smart wearables [16], etc. Among these LPWA technologies, LoRa has a relatively faster pace in technological development and commercialization. Hence in this paper, LoRa, as the representative LPWA technology, is applied into V2X communication networks.

LoRa is one of the most promising wide-area IoT technologies patented by Semtech and further promoted by the LoRa Alliance [10]. LoRa is based on chirp spread spectrum (CSS) modulation and is able to provide adaptive data rate and wide communication coverage but with low power consumption. Since the chirp pulse is relatively broadband, LoRa is good at resisting against multipath fading and Doppler shift. This helps to make LoRa ideal for mobile data communications, where multipath fading and Doppler shift coexist [17]. Semtech states that LoRa is able to support many applications of ITS [18], such as fleet management, asset tracking, fleet tracking, and smart parking, and etc.

Current traditional communication technologies in ITS [19] usually include Radio Frequency Identification (RFID), Bluetooth, ZigBee, WiFi, WAVE DSRC, 2G/3G/4G cellular networks, and etc. Compared with these communication technologies, LoRa is able to support a larger amount of devices up to millions per cell and cover longer communication range up to 10 km on the ground [20]. Unlike the traditional ITS communication technologies, usually mesh or ad-hoc topology, LoRa is based on the star topology where end nodes are directly connected to a gateway that relays data to a LoRa server. This significantly simplifies the network design allowing for higher scalability and greater controllability. Up to now, there have been some literatures study using LoRa for some ITS applications. In [21], the authors conducted an experimental study to evaluate LPWAN in both indoor and outdoor mobile environments. In [22], a vehicle monitoring system based on the LoRa technology was introduced. In [23], the authors proposed a LoRa-based LPWAN vehicle

¹Yuke Li and Linyao Yang are with The State Key Laboratory for Management and Control of Complex Systems, Institute of Automation, Chinese Academy of Sciences, Beijing 100190, China, Qingdao Academy of Intelligent Industries, Qingdao 266109, China, and also with School of Computer and Control Engineering, University of Chinese Academy of Sciences, Beijing 100049, China. liyuke2014, yanglinyao2017@ia.ac.cn

²Shuangshuang Han is with The State Key Laboratory for Management and Control of Complex Systems, Institute of Automation, Chinese Academy of Sciences, Beijing 100190, China, Qingdao Academy of Intelligent Industries, Qingdao 266109, China, and also with Qingdao Huituo Intelligent Machine Company, Qingdao, China. shuangshuang.han@ia.ac.cn

³Fei-Yue Wang is with The State Key Laboratory for Management and Control of Complex Systems, Institute of Automation, Chinese Academy of Sciences, Beijing 100190, China, and also with the Research Center for Military Computational Experiments and Parallel Systems Technology, National University of Defense Technology, Changsha 410073, China. feiyue.wang@ia.ac.cn

⁴Hui Zhang is with the Computer Science Department, School of Computer Science, Carnegie Mellon University, Pittsburgh, PA 15213, USA and also with Conviva Inc., Silicon Valley, CA 94404, USA. hzhang@conviva.com

diagnostic system named i-car system to improve the driving safety. Nevertheless, despite the increasing popularity of research in LoRa, little is known about the performance of LoRa operated in V2X communication scenarios.

To fill this knowledge gap, in this paper we select several LoRa schemes with different parameter configurations, and then evaluate their bit error performance (BER) correspondingly under six typical V2X communication scenarios. The major contributions of this paper can be summarized on two aspects: On the one hand, we are the first to apply LoRa to V2X communications, then evaluate, analyze, and characterize the performance of LoRa in six scenarios containing both V2I and V2V situations with a wide range of Doppler shifts. On the other hand, based on the simulation results and analysis, some suggestions are derived about how to select the parameter configurations of LoRa to obtain better performance in mobile scenarios.

This paper is organized as follows. In Section II, we present a brief review of the LoRa technology and introduce the key parameters for customization of LoRa. In Section III, the details of the channel model is presented, and a comparison between the coherence time of six scenarios and the symbol time of different LoRa schemes is demonstrated. In Section IV, the simulation results and analysis are presented and discussed. Finally, Section V concludes this paper.

II. LORA BASICS

LoRa is a proprietary spread spectrum modulation technique designed and patented by Semtech. Technically, LoRa can commonly refer to two distinct layers: (i) a physical layer using the CSS radio modulation technique; and (ii) a MAC layer protocol (LoRaWAN), which is optimized specifically for energy limited end devices [24].

A. The LoRa Modulation

LoRa is based on chirp spread spectrum scheme that uses wideband linear frequency-modulated pulses whose frequency decreases or increases over a specific amount of time based on the encoded information. Because of sufficiently broadband chirps, the robustness against multipath fading is improved. Radio signals of LoRa are able to resist against in-band and out-of-band interference with the help of high-bandwidth-time production, which contributes to the maximum link budget of about 157 dB and henceforth provides good coverage [25].

A LoRa radio has four parameters for the customization of the modulation: carrier frequency, spreading factor, bandwidth and coding rate. The selection of these parameters determines energy consumption, transmission range and resilience to noise.

Carrier frequency: Carrier frequency is the centre frequency used for the transmission band. LoRa operates in the lower industrial, scientific, and medical (ISM) bands (EU: 868MHz and 433 MHz, USA: 915MHz and 433 MHz). In this paper, we address the operation in the EU ISM 868 MHz band.

Spreading factor (SF): The LoRa modulation employs six orthogonal SFs ranging from 7 to 12 to implement

variable data rates and lengths in time. Modulated signals at different spreading factors appear as noise to the target receiver. This enables multiple different spread signals to be transmitted at the same time and on the same frequency channel without degrading the communication performance and trading the on-air time for the communication range. With this design, the spectral efficiency and the network capacity are significantly improved.

Bandwidth (BW): The bandwidth is the most important parameter of the LoRa modulation. A LoRa symbol is composed of 2^{SF} chirps, which cover the entire frequency band. The different LoRa chip modules have different bandwidth settings: The SX1272 has three programmable bandwidth settings: 500 kHz, 250 kHz, and 125 kHz. The SX1276 can be programmed in the range of 7.8 kHz to 500 kHz.

Code rate (CR): CR is the forward error correction (FEC) rate used by the LoRa modem and offers protection against bursts of interference. Decreasing the code rate helps to reduce the Packet Error Rate (PER) in the presence of short bursts of interference but increases time on air. The code rate (CR) is calculated as $4/(4+n)$, where n is the parity bits and $n \in \{1, 2, 3, 4\}$. CR of the payload is stored in the header of the packet, which is always encoded at 4/8.

The symbol rate of LoRa, R_s , is defined as

$$R_s = \frac{BW}{2^{SF}} \quad (1)$$

The symbol period T_s is the reciprocal of R_s , derived by

$$T_s = \frac{1}{R_s} = \frac{2^{SF}}{BW} \quad (2)$$

Taking the code rate into account, as well as the fact that SF bits of information are transmitted per symbol, the nominal bit rate R_b of the data signal can be defined as:

$$R_b = SF \times \frac{BW}{2^{SF}} \times CR \quad (3)$$

From Eq. (1) to (3), a higher spreading factor increases transmission duration and decreases the data rate. With a given spreading factor, a doubling of the bandwidth can effectively double the transmission rate and halve the time on air, but lower the receiver sensitivity due to integration of additional noise. In addition, reducing code rate helps to decrease the PER in the presence of the short bursts of interference.

B. LoRaWAN

The second component is the LoRaWAN network protocol which is optimized specifically for energy limited end devices. LoRaWAN networks are operated using ALOHA in a star configuration. The end devices communicating with base stations called gateways or concentrators. Data are then conveyed to a network server before connected to end-user applications and servers. The star topology enables LoRa to transmit over very long distances. The MAC layer also defines three options for scheduling the receive window slots for downlink communication, which are named as classes A, B, and C, in which class A must be supported by the end



Fig. 1. Six time- and frequency-selective empirical channel models for V2X communications.

TABLE I
CHANNEL PARAMETERS

| Scenario | Velocity (km/h) | Doppler Shift (Hz) |
|------------|-----------------|--------------------|
| Scenario 1 | 104 | 1000-1200 |
| Scenario 2 | 32-48 | 300 |
| Scenario 3 | 104 | 900-1150 |
| Scenario 4 | 104 | 600-700 |
| Scenario 5 | 32-48 | 400-500 |
| Scenario 6 | 32-48 | 300-500 |

devices. The details about the LoRaWAN protocol can be found in [24].

III. CHANNEL MODEL AND ANALYSIS

In the simulations of this paper, we use the channel model proposed in [26] [27], which is typically regarded as a standard V2X channel model dedicated for IEEE 802.11p standard. The measurement campaign was carried out in the metropolitan Atlanta, Georgia area including six scenarios [28], as shown in Fig. 1, which are

- Scenario 1: V2V Expressway Oncoming;
- Scenario 2: V2V Expressway Same Direction with Wall;
- Scenario 3: V2V Urban Canyon Oncoming;
- Scenario 4: Roadside-to-vehicle (R2V) Expressway;
- Scenario 5: R2V Urban Canyon Oncoming;
- Scenario 6: R2V Suburban Street.

The channel parameters for these six scenarios are listed in Table I. We can see that the Scenarios 1-6 cover both V2V and R2V channels and a wide range of Doppler shifts.

By the nature of LoRa physical layer design using the linearity of chirp pulses, frequency offsets between the receiver and the transmitter are equivalent to timing offsets, easily eliminated in the decoder, which makes LoRa equipped with the ability of resisting against the Doppler effect [29]. In next subsection, this ability is further explored and analyzed when faced with various V2X scenarios.

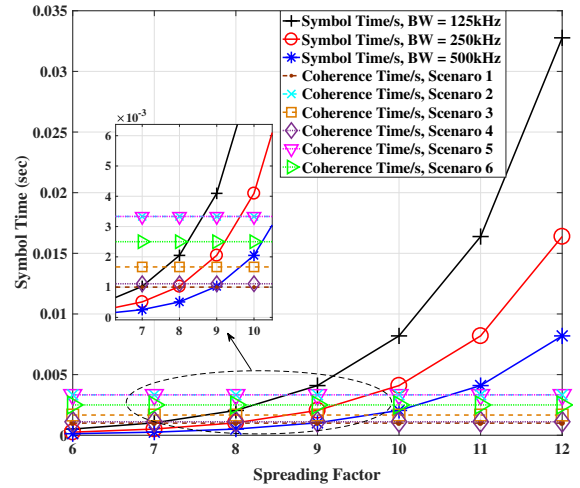


Fig. 2. The comparison between coherence time T_c of six scenarios and symbol time T_s of LoRa with all specifications.

A. Doppler Effect

Doppler shift in mobile channels causes a small frequency shift in LoRa pulse and introduces a shift in the time axis of the baseband signal. To inspect the Doppler effect on LoRa when transmitted in V2X channels, the channel coherence time (T_c) and symbol time (T_s) should be compared.

Coherence time is inversely proportional to Doppler shift as

$$T_c = \frac{1}{f_D} \quad (4)$$

The symbol time of LoRa is shown in (2). From (2), we can see that T_s increases as SF increases or BW decreases. When the symbol time of LoRa is larger than the coherence time, i.e. $T_s > T_c$, the amplitude and phase change are imposed by the channel varies considerably during the transmission. This is the phenomenon of fast fading, which makes accurately estimate or equalize the channel become very difficult [30].

TABLE II
SYSTEM PARAMETERS

| Parameter | Value |
|-------------------|----------------------|
| Spreading Factor | 7, 10 |
| Signal Bandwidth | 125kHz, 500 kHz |
| Carrier Frequency | 870 MHz |
| Sample Interval | 8 μ s, 2 μ s |
| Code Rate | 1 |

In order to clearly see when the fast fading occurs in our simulation, the comparison between the symbol time with different SF and BW and the coherence time of six scenarios are shown in Fig. 2.

From Fig. 2, we observe that when $SF = 7$, T_c of six scenarios are all larger than T_s with all shown BW s. As SF increases, T_s raises exponentially. Only partial scenarios T_c are larger than T_s with specific BW s, e.g., when $SF = 9$, only for scenarios 2, 5, and 6, T_c of these scenarios are larger than T_s with $BW = 250$ and 500 kHz. When SF is larger than 10, T_c of six scenarios are all smaller than T_s with all BW specifications, in which the fast fading occurs and induces the signal distortion. In order to avoid fast fading, when $BW = 500$ kHz, SF of LoRa should be set to be less than 9 so that T_c is larger than T_s . When $BW = 250$ kHz, SF should be set less than 8 and when $BW = 125$ kHz, SF should be set less than 7.

In order to clearly see how the Doppler effect acts on the performance of LoRa, in next section we carry out Monte Carlo simulation to analyze the performance of LoRa applied in aforementioned six V2X communication scenarios. The performance of LoRa schemes with various parameter specifications are also evaluated.

IV. SIMULATION RESULTS

In this section, we carry out Monte Carlo simulations to analyze the BER performance of LoRa versus the signal-to-noise ratio (SNR). The simulations are carried out at the link level. All of the simulation parameters are selected according to the LoRa specifications. In order to learn about which parameter configurations of LoRa show better performance in V2X channels, we select three LoRa configuration schemes to examine their BER performance, as follows:

- Scheme 1: $SF = 7$, $BW = 500$ kHz;
- Scheme 2: $SF = 7$, $BW = 125$ kHz;
- Scheme 3: $SF = 10$, $BW = 500$ kHz.

The carrier frequency is operated in European ISM 863-870 MHz band. For simplicity, the channel coding is omitted and CR is set to be 1. The simulation system parameters are listed in Table II.

In our simulations, the channel estimation is performed based on the preamble, which is located prior to each data symbol and comprises an entire symbol known by both the transmitter and the receiver. Then, the channel estimates are used for the equalization and demodulation of the data symbol. The channel equalization algorithm is zero-forcing. We detect the received LoRa symbols by a cyclic correlator receiver, which is described in detail in the patent [31].

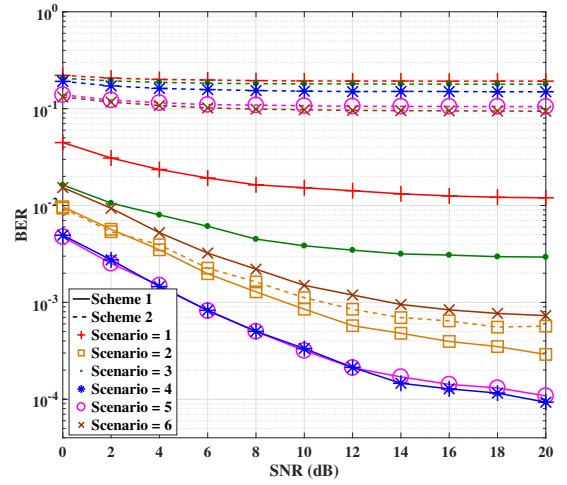


Fig. 3. The comparison between Scheme 1 and Scheme 2 under six V2X scenarios.

Fig. 3 shows the performance comparison between Scheme 1 and Scheme 2 under six V2X scenarios. From Fig. 3, scenario 1 shows the worst BER performance than other scenarios due to the highest Doppler shift. It also can be observed that Scheme 1 outperforms Scheme 2 for both V2V and R2V scenarios. When SNR = 0, BERs of Scheme 1 with most of scenarios exhibit around 10^{-2} . As SNR increases, BERs of Scheme 1 exhibits lower than 10^{-3} . As for Scheme 2, the BER performance exhibits error floor in the entire SNR region under most of scenarios. The reason is that the larger BW of Scheme 1 contributes to a much smaller symbol time than Scheme 2, which is lower than coherence time of channels (see in Fig. 2). Thus, the possibility of the Doppler-induced signal distortion occurred on Scheme 1 is much smaller than that of Scheme 2. For Scheme 2, the fast fading caused by Doppler shift as well as the intersymbol interference (ISI) signals caused by delay spread both exert pressures on Scheme 2, which in turn seriously deteriorate its performance.

The performance comparison between Scheme 1 and Scheme 3 is given in Fig. 4. In this figure, Scheme 3 with higher SF of 10 shows worse BER performance than Scheme 1 and exhibits error floor in the entire SNR region even in scenario 6 that is equipped with the lowest velocity and Doppler shift. This happens because according to Eq. (2), with given BW , each increase in SF doubles transmission duration, thus the transmission duration of Scheme 3 is triple to Scheme 1 and comparable to the coherence time (see in Fig. 2), which triggers the fast fading.

Remarks: In order to combat fast fading caused by Doppler shift, the most direct way is to reduce the symbol time until it is lower than the coherence time of channel. By this way, the amplitude and phase change imposed by the channel can be considered roughly constant over the period of transmission. As a result, it is suggested that LoRa schemes with higher BW and lower SF parameter specifications should be selected to obtain better performance when applied in V2X communication scenarios. However,

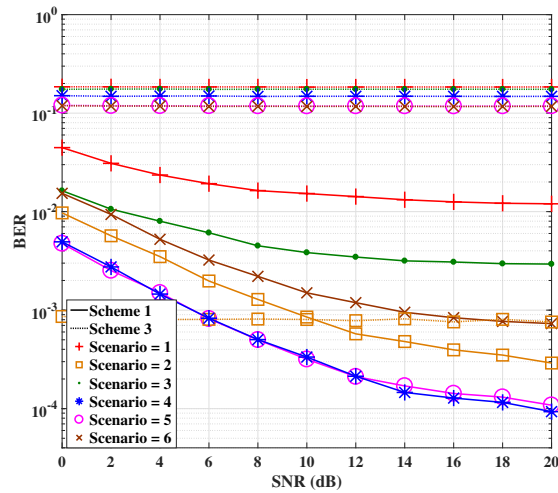


Fig. 4. The comparison between Scheme 1 and Scheme 3 under six V2X scenarios.

LoRa schemes with higher SF may lose their superiority in communication coverage [20]. Channel coding and interleaving techniques are also alternative approaches for LoRa to conflict the time-selective fading in mobile scenarios.

V. CONCLUSIONS

In this paper, we applied LoRa in V2X communications and evaluated the BER performance of LoRa schemes with different parameter specifications under six V2X scenarios including both V2I and V2V channels. Simulation results showed that LoRa schemes with the longer symbol time exhibit worse BER performance and even error floor under most of scenarios due to the impact of the fast fading. Consequently, it is suggested that higher BW and lower SF parameter configurations should be selected to resist against the fast fading caused by Doppler effect when LoRa was applied in V2X communications.

ACKNOWLEDGMENT

This work was supported partly by the National Natural Science Foundation of China 61501461, 61702519, and 61533019; and the Early Career Development Award of SKLMCCS (Y3S9021F34).

REFERENCES

- [1] N. Lu, N. Cheng, N. Zhang, X. Shen and J. W. Mark, "Connected Vehicles: Solutions and Challenges," *IEEE Internet of Things J.*, vol. 1, no. 4, pp. 289-299, Aug. 2014.
- [2] F.-Y. Wang, N.-N. Zheng, D. P. Cao, C. M. Martinez, L. Li, and T. Liu, "Parallel driving in CPSS: a unified approach for transport automation and vehicle intelligence," *IEEE/CAA J. of Autom. Sinica*, vol. 4, no. 4, pp. 577-587, Oct. 2017.
- [3] H. Y. Guo, D. P. Cao, H. Chen, C. Lv, H. J. Wang, and S. Q. Yang, "Vehicle dynamic state estimation: state of the art schemes and perspectives," *IEEE/CAA J. of Autom. Sinica*, vol. 5, no. 2, pp. 418-431, Mar. 2018.
- [4] S. Han, F.-Y. Wang, Y. Wang, D. Cao and L. Li, "Parallel Vehicles based on the ACP theory: Safe trips via self-driving," in *Proc. 2017 IEEE Intell. Vehicles Symp. (IV)*, Los Angeles, CA, 2017, pp. 20-25.
- [5] F.-Y. Wang, X. Wang, L. Li, and L. Li, "Steps toward parallel intelligence," *IEEE/CAA J. of Autom. Sinica*, vol. 3, no. 4, pp. 345-348, Oct. 2016.

- [6] F.-Y. Wang, L. Yang, X. Hu, X. Cheng, S. Han, and J. Yang, "Parallel networks and network softwarization: a novel network architecture (in chinese)," *Sci Sin Inform.*, vol. 47, pp. 1-21, 2017.
- [7] F.-Y. Wang, L. Yang, X. Cheng, S. Han, and J. Yang, "Network softwarization and parallel networks: beyond software-defined networks," *IEEE Network*, vol. 30, no. 4, pp. 60-65, Jul. 2016.
- [8] F.-Y. Wang, "Computational Social Systems in a New Period: A Fast Transition Into the Third Axial Age," *IEEE Trans. on Computational Social Syst.*, 2017, vol. 4, no. 3, pp. 52-53.
- [9] F.-Y. Wang, "The emergence of intelligent enterprises: From CPS to CPSS," *IEEE Intell. Syst.*, vol. 25, no. 4, pp. 85-88, July 2010.
- [10] LoRa Alliance. [Online]. Available: <https://www.lora-alliance.org/>
- [11] Sigfox. [Online]. Available: <https://www.sigfox.com/>
- [12] Y. P. E. Wang et al., "A Primer on 3GPP Narrowband Internet of Things," *IEEE Commun. Mag.*, vol. 55, no. 3, pp. 117-123, March 2017.
- [13] Ingenu. [Online]. Available: www.ingenu.com/
- [14] M. Centenaro, L. Vangelista, A. Zanella and M. Zorzi, "Long-range communications in unlicensed bands: the rising stars in the IoT and smart city scenarios," *IEEE Wireless Commun.*, vol. 23, no. 5, pp. 60-67, October 2016.
- [15] Y. Li, X. Cheng, Y. Cao, D. Wang and L. Yang, "Smart Choice for the Smart Grid: Narrowband Internet of Things (NB-IoT)," *IEEE Internet of Things J.*, vol. PP, no. 99, pp. 1-1.
- [16] J. Petäjäjärvi, K. Mikhaylov, M. Hämäläinen and J. Iinatti, "Evaluation of LoRa LPWAN technology for remote health and wellbeing monitoring," in *Proc. 2016 10th Int. Symp. Medical Inform. and Commun. Technol. (ISMICT)*, Worcester, MA, 2016, pp. 1-5.
- [17] LoRa™ Modulation Basics, Application Note, Semtech, AN1200.
- [18] LoRa Applications. [Online]. Available: <https://www.semtech.com/technology/lora/lora-applications>
- [19] A. Maimaris and G. Papageorgiou, "A review of Intelligent Transportation Systems from a communications technology perspective," in *Proc. 2016 IEEE 19th Int. Conf. Intell. Transp. Syst. (ITSC)*, Rio de Janeiro, 2016, pp. 54-59.
- [20] J. Petäjäjärvi, K. Mikhaylov, A. Roivainen, T. Hanninen and M. Petäjäjärvi, "On the coverage of LPWANs: range evaluation and channel attenuation model for LoRa technology," in *Proc. 2015 14th Int. Conf. ITS Telecommun. (ITST)*, Copenhagen, 2015, pp. 55-59.
- [21] D. Patel and M. Won, "Experimental Study on Low Power Wide Area Networks (LPWAN) for Mobile Internet of Things," in *Proc. 2017 IEEE 85th Veh. Technol. Conf. (VTC Spring)*, Sydney, NSW, 2017, pp. 1-5.
- [22] Hsieh, Chao-Linag, et al. "A Vehicle Monitoring System Based on the LoRa Technique," *Int. J. of Mech., Aerospace, Ind., Mechatronic and Manufacturing Eng.*, vol. 11, no. 5, pp. 1004-1010, 2017.
- [23] Y. S. Chou et al., "i-Car system: A LoRa-based low power wide area networks vehicle diagnostic system for driving safety," in *Proc. 2017 Int. Conf. Applied Syst. Innovation (ICASI)*, Sapporo, 2017, pp. 789-791.
- [24] N. Sornin, M. Luis, T. Eirich, T. Kramp, and O. Hersent, "LoRaWAN Specifications," LoRa Alliance, 2015.
- [25] J. Petäjäjärvi, Juha, et al. "Performance of a low-power wide-area network based on LoRa technology: Doppler robustness, scalability, and coverage," *Int. J. of Distributed Sensor Networks*, vol. 13, no. 3, Mar. 2017.
- [26] X. Cheng, M. Wen, L. Yang and Y. Li, "Index modulated OFDM with interleaved grouping for V2X communications," in *Proc. 17th Int. IEEE Conf. Intell. Transp. Syst. (ITSC)*, Qingdao, 2014, pp. 1097-1104.
- [27] Y. Li, M. Wen, X. Cheng and L. Q. Yang, "Index modulated OFDM with ICI self-cancellation for V2X communications," in *Proc. 2016 Int. Conf. Comput. Networking and Commun. (ICNC)*, Kauai, HI, 2016, pp. 1-5.
- [28] Guillermo Acosta-Marum and M. A. Ingram, "Six time- and frequency- selective empirical channel models for vehicular wireless LANs," *IEEE Veh. Technol. Mag.*, vol. 2, no. 4, pp. 4-11, Dec. 2007.
- [29] Augustin, Aloijs, Jiazi Yi, Thomas Clausen, and William Mark Townsley, "A study of LoRa: Long range & low power networks for the internet of things," *Sensors*, vol. 16, no. 9, 1466, 2016.
- [30] Rappaport TS, "Mobile radio propagation: small-scale fading and multipath," in *Wireless commun.: principles and practice*, Vol. 2. New Jersey: prentice hall PTR, 1996, pp.139-196.
- [31] Hiscock, Paul Dominic. "Chirp modulation." U.S. Patent No. 8,971,379. 3, Mar. 2015.